Journal of the European Ceramic Society 21 (2001) 2521–2533

www.elsevier.com/locate/jeurceramsoc

Conversion of Al_2O_3–SiO_2 powder mixtures to 3:2 mullite following the stable or metastable phase diagram

H.-J. Kleebe*[,1], F. Siegelin[2], T. Straubinger[3], G. Ziegler

University of Bayreuth, Institute for Materials Research (IMA I), D-95440 Bayreuth, Germany

Abstract

A model system, composed of powder blends of amorphous isomorphic silica spheres, being 500 nm in diameter, and also monosized crystalline α-Al_2O_3 powder, was investigated. Two different particle sizes of the corresponding alumina powder were employed: 300 nm and 2 μm. This particular assembly enabled a distinction between amorphous silica and crystalline alumina merely by their difference in particle morphology. The powder blends were sintered at temperatures between 1400 and 1700°C and the microstructure evolution was characterized by scanning (SEM) and transmission electron microscopy (TEM). It is worth noting that upon annealing at 1700°C, both microstructures were indistinguishable. However, depending on the Al_2O_3 particle size, different conversion mechanisms were monitored. When using the 300 nm Al_2O_3 powder, fast dissolution of alumina into the coalesced silica glass occurred, followed by homogeneous nucleation and growth of mullite within the glass. Utilizing 2 μm Al_2O_3 particles, however, resulted in the formation of two Al-containing glasses (phase separation into a Si- and Al-rich glass). In this case, the transformation to mullite can be rationalized by the conversion of the metastable Al-rich transient glass into mullite, which forms an epitaxial, single crystalline coating on the host Al_2O_3 particle. Therefore, depending on the initial Al_2O_3 particle size, mullite formation follows either the stable or metastable phase diagram.

Keywords: Al_2O_3–SiO_3; Mullite

1. Introduction

In contrast to the Al–Si-oxides sillimanite, andalusite, and cyanite, mullite, $3Al_2O_3{\cdot}2SiO_2$, is the only one compound in the binary Al_2O_3–SiO_2 system which is stable in contact with a liquid at high temperatures.[1,2] Because of its promising thermo-mechanical properties like low thermal expansion, low thermal conductivity, excellent creep resistance, and good chemical and oxidation resistance, mullite is a promising candidate for advanced structural and functional ceramics.[3–8] Moreover, glass-free, pure mullite has been reported to retain its room-temperature strength up to 1500°C.[9–11]

Over the last decades, a number of different mullite synthesis techniques, starting either from naturally occurring alumino-silicates or synthetic molecular precursors, have been described in literature.[12–18] However, as reported by Bowen and Greig,[2] mullite was first synthesized unknowingly as long ago as 1865 by Sainte-Claire Deville and Caron, who passed SiF_4 over a mixture of alumina and silica at a bright red heat and obtained crystals that had the composition close to 3:2 mullite. Bowen and Greig repeated this experiment in 1924 and yielded crystals that showed refractive indices identical with those of pure mullite.

Regarding more recent developments in processing techniques, the sol-gel approach is one of the many possible routes to obtain dense mullite ceramics.[12] In comparison to the conventional powder route, its main advantages are the lower temperatures required for densification and the possibility to produce high-purity materials. Sol-gel precursors to produce mullite are usually divided into two general categories: (i) single-phase and (ii) diphasic gels.[13,14] Single-phase systems have a molecular scale of mixing of Al- and Si-ions and crystallize rapidly by a strong exothermic reaction slightly below 1000°C. The nucleation-controlled reaction has an activation energy of ≈300 kJ/mol. Diphasic gels show a segregation of Al- and Si-rich precursor on a rather fine scale (≈2–100 nm) and reveal only a weakly exothermic reaction at about 1150–1350°C.[15–17]

* Corresponding author.
E-mail address: hkleebe@mines.edu (H.-J. Kleebe).
[1] Now at: Colorado School of Mines, Metallurgical and Materials Engineering Department, Golden, CO 80401, USA.
[2] Now at: Infineon Technologies AG, D-81609 Munich, Germany.
[3] Now at: University of Erlangen, Institute for Materials Science VI, D-91058 Erlangen, Germany.

0955-2219/01/$ - see front matter
PII: S0955-2219(01)00275-8

Kara et al.[18] have studied microstructures of mullites produced by reaction sintering of diphasic sol-gel derived mixtures from pseudoboehmite or colloidal aluminum sulfate with silica. Mullite formation takes place at 1275°C, which is consistent with observations from Wei and Halloran[17] on stoichiometric diphasic gels, who studied the phase transformation behavior in gels prepared from colloidal boehmite and tetraethylorthosilicate (TEOS). They observed a temperature-dependent incubation period prior to mullite formation. This incubation stage is followed by a rapid nucleation event and subsequent mullite growth from a constant nuclei density. Li and Thomson also studied mullitization of diphasic gels prepared from colloidal boehmite and TEOS.[19] They reported activation energies which are in agreement with those obtained by Wei and Holleran.[17] Similarly, Sundaresan and Aksay concluded that rapid mullite nucleation and subsequent growth occurred within the siliceous glass phase.[20]

There are only few detailed studies on mullite formation using diphasic powders in which the alumina source is α-Al_2O_3. Sacks et al.[21–23] have studied densification and transformation behavior during heat treatment of submicrometer composite particles that consisted of α-Al_2O_3 cores ($\approx$180 nm Ø) and amorphous silica coatings (TEOS) by differential thermal analysis (DTA), X-ray diffractometry (EDX), and scanning electron microscopy (SEM). Chemical composition of those diphasic powders was adjusted by simply changing the thickness of the amorphous silica coat. These powder compacts were viscously sintered to almost full density at around 1300°C and subsequently converted to mullite during annealing at temperatures $\geqslant$1400°C. Similar to Wei and Halloran[17] they reported an incubation period prior to mullitization. Rapid mullite growth occurred in the initial 1st growth stage and is followed by a 2nd stage of slower mullite growth. Their study provided evidence that the reaction rate during the 1st stage of mullite formation is controlled by dissolution of Al_2O_3 in the siliceous phase. The same rate controlling step was proposed by Huling and Messing[15] and Sundaresan and Aksay[20] for mullitization of diphasic sol-gel materials. Moreover, they found that the 2nd stage of mullitization reaction was highly dependent on the composition. The reaction was completed at a much lower temperature in both alumina- and silica-rich samples, as compared to a near stoichiometric composition, because shorter diffusion distances were affective in both non-stoichiometric samples.

In contrast to the sol-gel and/or composite route described above, less studies were performed on mullite formation via reaction sintering of crystalline SiO_2 and α-Al_2O_3. Wahl et al. were first to systematically investigate reaction sintering of mullite by means of high-temperature X-ray diffraction, employing different alumina and silica sources.[24] Scanning electron microscopy studies of microstructure evolution of mullite polycrystals processed by reaction sintering of different SiO_2 materials and α-Al_2O_3 was examined by Nurishi and Pask[25] and Rana et al.[26] Liquid-phase formation was observed prior to mullitization in the temperature range of 1300–1500°C. In the binary system α-Al_2O_3-cristobalite, liquid formation was rationalized by the metastable eutectic of the Al_2O_3–SiO_2 phase diagram,[27] while in quartz-containing mixtures, liquid formation was thought to be a result of the quartz$\Rightarrow$cristobalite transformation.[28] Johnson and Pask showed that the locus of mullitization lies right at the interface between liquid phase and crystalline Al_2O_3 (corundum)[29] and the subsequent growth of the mullite layer was governed by Al^{3+} and Si^{4+} interdiffusion. Schmücker et al.[30] studied mullitization during reaction sintering of quartz and α-Al_2O_3 powders by transmission electron microscopy. They reported that the reaction sequence starts with the formation of a transient glass phase on the surface of quartz grains. This viscous silica melt penetrates into α-Al_2O_3 agglomerates and simultaneously incorporates Al by dissolution of α-Al_2O_3. Nucleation of mullite was observed to occur mainly at the α-Al_2O_3/silica melt contact. In some instances, however, precipitation of mullite within residual glass pockets was observed. Growth of mullite was reported to proceed via interdiffusion of Al^{3+} and Si^{4+} species. Nucleation of mullite was rationalized by Al_2O_3 dissolution in the silica glass until a critical Al-concentration was reached. When exceeding this concentration, c_c, spontaneous, heterogeneous nucleation at the SiO_{2am}–α-Al_2O_3 interface was assumed. In contrast, Rana et al.[26] and Johnson and Pask[29] explained the incorporation of alumina into the siliceous melt by simultaneous growth and dissolution of preexisting mullite crystals, which were formed at the α-Al_2O_3 interface. However, it was argued by Schmücker et al.[30] that mullite formation prior to Al_2O_3 saturation of the melt can only be expected, when dissolution of corundum occurs faster than diffusion of Al^{3+} species inside the viscous glass, which had never been observed.

Takamori and Roy[31] studied the crystallization behavior of Al_2O_3-rich glasses, which were prepared by flame spraying and/or splat-cooling, by DTA, transmission electron microscopy (replica technique), and XRD. They found that the mullite crystallite size immediately after rapid crystallization increased continuously. All glasses studied with an Al_2O_3 content $>20\%$ showed the phenomenon of rapid crystallization at a reproducible temperature. They also concluded that the evidence for the existence and especially the location of a metastable glass-in-glass miscibility gap, reported in literature, is inadequate.

The goal of the present study is first to answer the question whether there is an Al_2O_3 particle size dependence of the $3Al_2O_3 + 2SiO_2 \Rightarrow$mullite conversion mechanism and, secondly, if the above mentioned transient viscous flow

mechanism is also affective in our model system. Therefore, powder blends were annealed at temperatures between 1300 and 1700°C and the respective samples (interrupted sintering cycles) were characterized by scanning and transmission electron microscopy. In addition, we addressed the question whether the stable and/or metastable phase diagram is applicable to describe mullitization.

2. Experimental procedures

A model system, composed of monosized powder blends of amorphous silica spheres ($d = 500$ nm) and monosized crystalline α-Al_2O_3 powder (corundum; Sumitomo Chemical Co., Ltd., Tokyo, Japan), with a particle size of either 300 nm (AA-04, which will be referred to as a fine-grain system) and 2 μm in diameter (AA-02, in the following denominated as a coarse-grain system), was employed in this study, as shown in Fig. 1. The advantage of this model system is, in particular, that a distinction between alumina and silica particles is possible simply by imaging, which is advantageous e.g. for in situ SEM hot-stage experiments that do not allow the use of the EDX detector. The amorphous silica spheres used here were prepared by hydrolysis and condensation of tetraethylorthosilicate (TEOS) in water/ammonia and ethanol mixtures.[32,33] The SiO_2 and the respective Al_2O_3 powder were dispersed in water with a weight fraction of 21 wt.% SiO_2 + 79 wt.% Al_2O_3, which corresponds to stoichiometric 3:2 mullite. Both powder mixtures were dried (80°C) and subsequently cold-pressed (20 MPa, 10 min) and sintered at different temperatures for various times (1300°C/0.5 h; 1400°C/0.5 h; 1500°C/0.5 and 4 h; 1600°C/0.5 h; 1700°C/0.5 h). Identification of the crystalline phases formed during sintering was performed by both XRD in an automatic powder diffractometer (Seifert XRD 300P, CuK_α radiation) and by selected area electron diffraction (SAD) during TEM observations. Changes of the microstructure in the early stages of conversion were monitored by scanning electron microscopy (SEM, Jeol 6400) on fracture surfaces in conjunction with TEM studies. Transmission electron microscopy (TEM) utilized a Philips CM20FEG (field emission gun) microscope fitted with an ultra-thin window Ge energy dispersed X-ray (EDX) detector. Operating at 200 kV, the instrument has a point resolution of 0.24 nm. TEM-foil preparation followed standard techniques involving cutting, ultra-sonic drilling, grinding, dimpling to a thickness of ≈10 μm, Ar-ion-beam thinning to perforation and thin carbon coating to minimize electrostatic charging in the microscope. During TEM studies, emphasis was put on the evaluation of the corresponding phase assemblage as well as the determination of the residual glass phase distribution within the matrix and along grain boundaries. Therefore, high-resolution transmission electron microscopy (HRTEM) was utilized.

3. Results

3.1. Fine-grain system

XRD patterns of the fine-grain system are shown in Fig. 2. Upon heat treatment at temperatures below

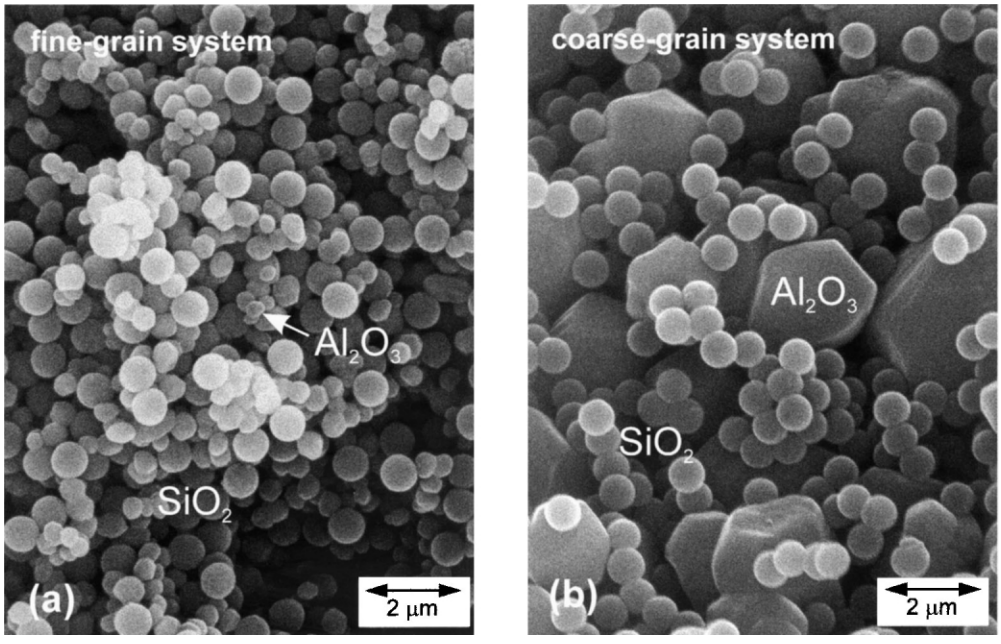

Fig. 1. SEM micrographs of the model systems employed, (a) fine-grain system composed of monosized, amorphous SiO_2 spheres (500 nm) and monosized α-Al_2O_3 particles being 300 nm in size, (b) coarse-grain system with the same silica spheres shown in (a) and faceted α-Al_2O_3 particles of 2 μm.

1500°C, no crystalline phase other than α-Al_2O_3 (corundum) was detected, indicating that silica is still in the non-crystalline state. The latter result is consistent with SEM observations of the fracture surface of powder blends annealed at 1300 and 1400°C, given in Fig. 3. While the microstructure at 1300°C does not reveal any major difference to the as-processed sample, heat treatment at 1400°C initiates coalescence of the silica spheres, which are, however, still amorphous. Thus, densification in this early stage of sintering occurs via the transient viscous sintering mechanism described by Sacks et al.[21] The characteristic of this sintering mechanism is that the amorphous siliceous phase starts to melt and allows for particle rearrangement and densification via viscous flow of SiO_2, before the conversion reaction takes place. At 1500°C/0.5 h, cristobalite forms followed by crystallization of mullite at 1500°C/4 h. At 1600°C, mullite and residual alumina are the only two crystalline phases detected, while at 1700°C/0.5 h, mullitization has strongly progressed. Apart from mullite, only minor traces of residual Al_2O_3 were detected at such high sintering temperature [see also Fig. 5 (a)].

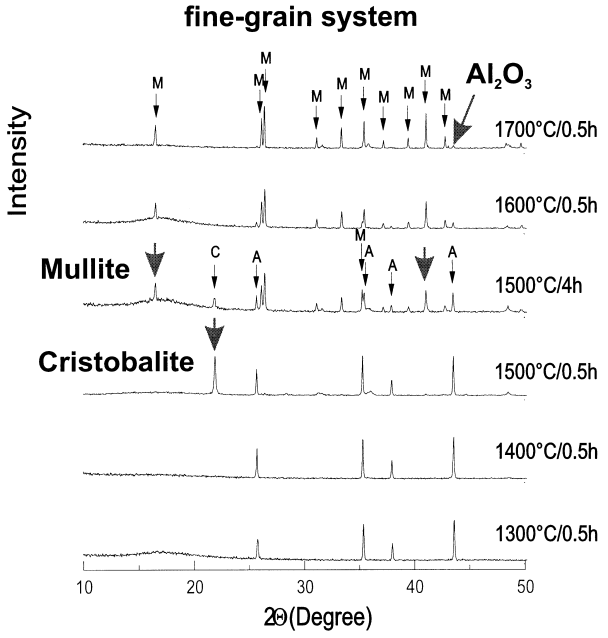

Fig. 2. XRD spectra of the fine-grain system sintered at temperatures ranging between 1300°C, 0.5 h and 1700°C, 0.5 h. Here, cristobalite was observed after annealing at 1500°C, 0.5 h, while traces of mullite were first detected at 1500°C, 4h. At 1700°C, mullitization is completed. Note that a small amount of alumina is still present in the dense high-temperature sample [compare also Fig. 5(a)].

Heat treating the fine-grain system at 1500°C for 1 h revealed Al_2O_3 grains, with almost no change in particle diameter, surrounded by an amorphous siliceous phase [see TEM image in Fig. 4 (a)]. The non-crystallinity of the surrounding phase could be confirmed by electron diffraction, since amorphous materials typically show a broad halo of elastically scattered electrons in contrast to distinct diffraction spots (Bragg condition), observed in crystalline samples. A homogenous distribution of a small Al-concentration in the amorphous phase was verified by EDX analysis. This finding is consistent with the HRTEM observation which showed that, although the overall morphology of the alumina particles did not

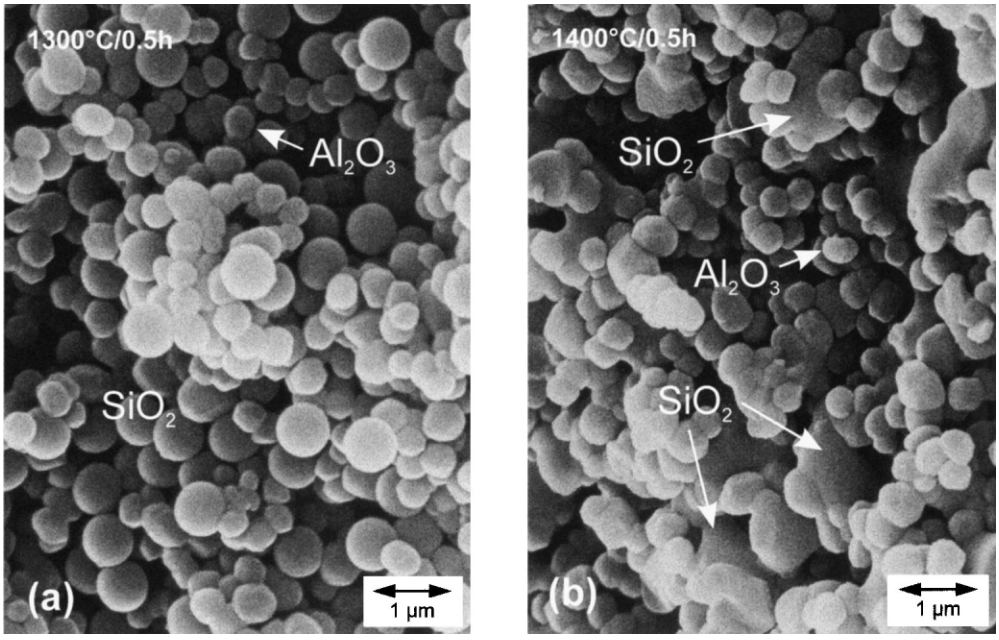

Fig. 3. SEM images of fracture surfaces (fine-grain system) after annealing at (a) 1300°C, 0.5 h and (b) 1400°C, 0.5 h. At 1300°C, no major difference between the annealed and as-processed sample was monitored. At 1400°C, predominantly coalescence of silica spheres was observed, which engulfs the fine Al_2O_3 particles (300 nm in diameter).

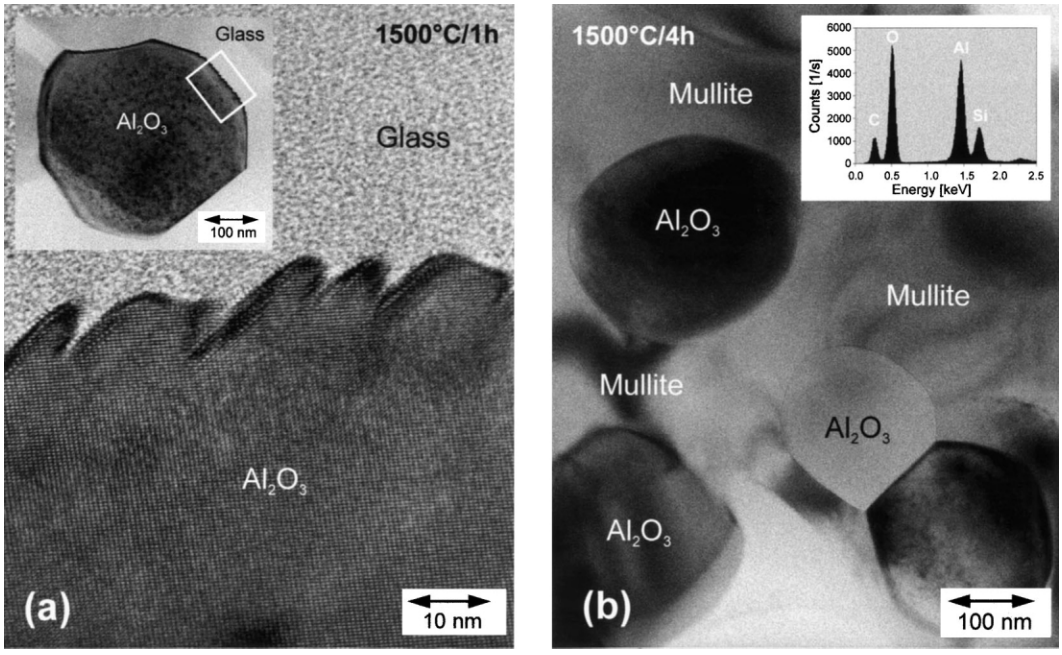

Fig. 4. TEM micrographs of the fine-grain system, (a) 1500°C, 1 h and (b) 1500°C, 4 h. As shown in (a), curved surfaces of alumina grains start to develop low-energy facets, which indicates the dissolution of Al_2O_3 in the siliceous phase. The inset (upper left corner) gives an overview of the whole Al_2O_3 grain. Upon 4 h annealing (b), extended regions of mullite were observed (see also EDX inset), engulfing alumina particles.

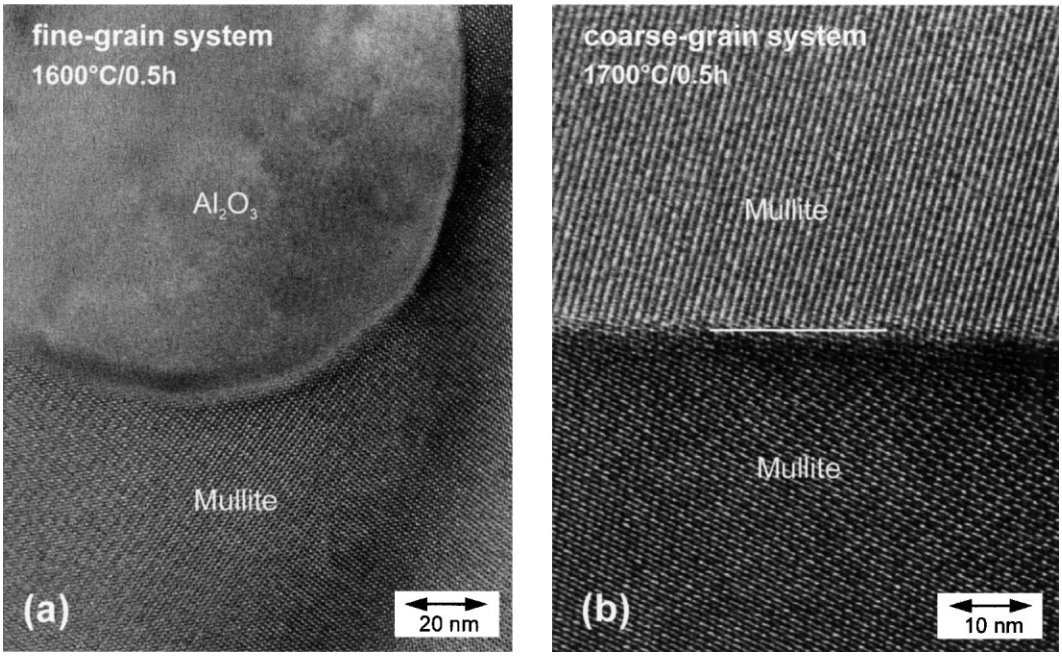

Fig. 5. HRTEM images of (a) the fine-grain system annealed at 1600°C, 0.5 h and (b) the coarse-grain system annealed at 1700°C, 0.5 h. At 1600°C, mullitization is nearly completed with, however, a higher amount of residual alumina, as shown in (a). Upon annealing at temperatures exceeding 1600°C, residual glass was neither observed at muli-grain junctions nor along mullite interfaces. Note that after densification at 1700°C, no distinction between the fine- and coarse-grain system was possible by TEM observations.

markedly change, initially round surface areas developed low-energy facets, indicating Al_2O_3 dissolution in the siliceous glass phase [Fig. 4 (a)].

At 1500°C/4 h, nearly complete conversion to 3:2 mullite has taken place and the microstructure is composed of rounded Al_2O_3 particles engulfed by large mullite grains [Fig. 4 (b)]. Only a few residual glass pockets were observed, which, however, had no direct contact to alumina particles but were adjacent to mullite grains. This observation suggests that during this stage of mullitization,

which in literature is generally referred to as the 2nd stage,[17,23] mullite growth proceeds via interdiffusion of alumina and silica.

Upon sintering at 1600°C/0.5 h, no residual glass was detected in the material, neither as isolated glass pockets nor as intergranular films along grain or phase boundaries. As a consequence of the interdiffusion process mentioned above, the size of the Al_2O_3 particles is reduced [compare Fig. 5(a)]. Increasing the sintering temperature to 1700°C/0.5 h, the mullite grain diameter is enlarged as a result of a higher interdiffusion rate. Apart from traces of alumina, also confirmed by XRD (Fig. 2), the fine-grain material is composed of 2–5 μm sized mullite grains, which showed a slightly higher Al-concentration compared to the sample annealed at 1600°C (EDX analysis). This result is in line with EELS data on sol-gel derived mullite reported by Kleebe et al.[34] They found that the Al-content of mullite grains slightly increased with increasing sintering temperature (curved phase field). Since only residual alumina and mullite were detected upon high-temperature annealing, the final bulk composition is slightly Al-rich, which (i) implies that some SiO_2 was lost during densification and (ii) explains that no amorphous intergranular film was observed at mullite interfaces. This latter observation is consistent with results obtained by Kara et al.,[18] who reported that the wetting/non-wetting behavior at grain-boundaries in reaction-sintered mullite ceramics depends on the respective bulk composition and thermal history of the material. It should be noted that Fig. 5 (b), in fact, reveals the high-temperature microstructure of the coarse-grain system, because both the fine- and coarse-grain material were indistinguishable by TEM inspection upon annealing at 1700°C. From the results given above it is concluded that the conversion mechanism in the fine-grain system follows the stable phase diagram, as schematically shown in Fig. 6. Fast dissolution of alumina in the amorphous siliceous phase favors homogeneous nucleation and growth of mullite within the residual glass (1st stage) followed by interdiffusion of Al_2O_3 and SiO_2 promoting continuous grain growth of mullite throughout the 2nd growth stage.

3.2. Coarse-grain system

The corresponding XRD spectra of the coarse-grain system are given Fig. 7. Similar to the fine-grain system, the only detectable crystalline phase at temperatures below 1400°C is α-Al_2O_3, which underlines that SiO_2 is still amorphous and densification also occurs here via transient viscous flow.[21] Formation of cristobalite was observed at a lower temperature compared to the fine-powder mixture, i.e. at 1400°C/0.5 h. Mullite formation was also first monitored at 1500°C/4 h (compare Fig. 2), however, to a much less volume fraction. Obviously, mullitization starts in both systems at about the same temperature, but with a different conversion rate. In contrast to the fine-grain system, cristobalite is here still present at 1600°C/0.5 h. Annealing at 1700°C results in a complete conversion to mullite. Also in this system, traces of corundum were monitored upon high-temperature sintering.

In Fig. 8, corresponding SEM and TEM images of the coarse-grain system annealed at 1400°C/0.5 h are given. It is interesting to note that the silica spheres showed less coalescence in this system, but instead formed hemispheres on the (large) alumina particles. In order to

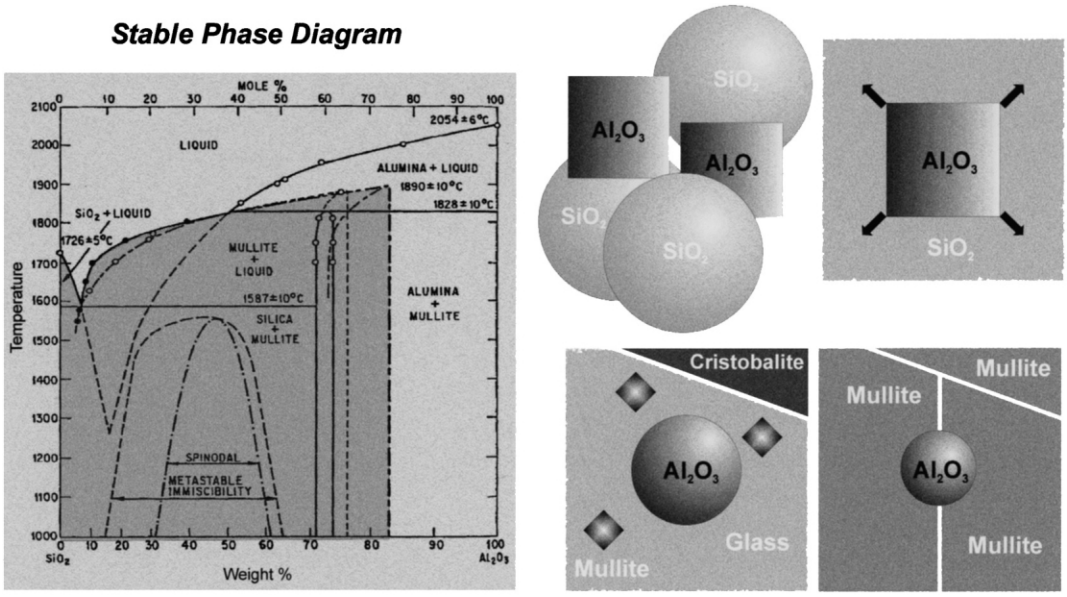

Fig. 6. Schematic illustrating the conversion mechanism of the fine-grain system (homogeneous nucleation), which follows the stable phase diagram (after Aksay and Pask, 1975);[36] for detailed information see text.

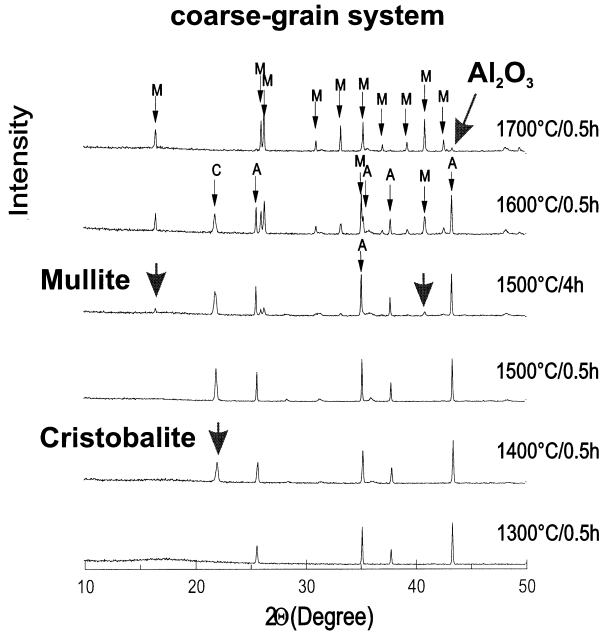

Fig. 7. XRD spectra of the coarse-grain system sintered at temperatures ranging between 1300°C, 0.5 h and 1700°C, 0.5 h. In contrast to the fine-grain system (see also Fig. 2), cristobalite was detected already at 1400°C, 0.5 h. Traces of mullite were also first detected at 1500°C, 4 h, however, to a less amount as compared to the fine-grain system. The XRD spectrum obtained at 1700°C, 0.5 h is identical to that shown for the fine-grain system (complete mullitization, traces of residual alumina).

verify whether SiO_2 diffused into the alumina particles, or a dissolution of Al_2O_3 into the amorphous silica phase changed the glass composition and consequently its wetting behavior (being responsible for the observed morphology change), EDX analysis in the TEM imaging mode was performed. As shown in Fig. 8(b), the SiO_2 hemispheres indeed contained a small fraction of aluminum.

At higher annealing temperature, i.e. 1500°C/0.5 h, these hemispheres are now composed of cristobalite coated by an Al-containing glass phase [see Fig. 9(a)]. Applying a longer holding time at constant sintering temperature (1500°C/1 h), a second, Al-rich glass phase develops right at the Al_2O_3/cristobalite phase boundary with a film thickness of ≈20–30 nm, as shown in the TEM image in Fig. 9(b); see also corresponding EDX inset. It is important to note that in the coarse-grain system, in contrast to the material processed with the fine Al_2O_3 powder, two different residual glass phases being Si- (SiO_2-hemisphere coating) and Al-rich (phase boundary) coexisted at 1500°C.

When extending the holding time to 4 h at 1500°C, only the Al-rich transient glass phase, formerly present at the Al_2O_3/cristobalite phase boundary, converted to a 30–50 nm thin, single crystalline mullite coat on Al_2O_3 grains. Note that no characteristic orientation relationship between Al_2O_3 and mullite epitaxial layer was observed. As shown in Fig. 10, this mullite coating nearly completely engulfs the alumina particles. In some instances, cristobalite could still be detected (compare also XRD spectra in Fig. 2). It should be noted that TEM imaging of cristobalite is rather difficult, since this crystalline phase is electron beam sensitive and readily transforms to amorphous silica.

Based on the above results, the mullite conversion mechanism in the coarse-grain system is schematically illustrated in Fig. 11. Also in this system, alumina first dissolves in the siliceous glass (formation of hemispheres) followed by the nucleation of cristobalite. Furthermore, the separation of the residual glass into two transient, metastable glass phases (Si-/hemisphere surface and Al-rich/phase boundary) was observed. At a longer holding time at temperature (1500°C/4 h), the Al-rich glass phase along the Al_2O_3/cristobalite phase boundary transforms into mullite. Therefore, it is concluded that the conversion mechanism of the coarse-grain system follows the metastable phase diagram. However, upon high-temperature annealing at 1700°/0.5 h mullitization is completed and both system reveal indistinguishable microstructures.

4. Discussion

Analyzing the XRD data, two major differences become obvious when comparing the fine- and coarse grain system: (i) cristobalite formation is retarded in the fine-grain system, i.e. in the coarse-grain system, cristobalite was detected at a about 100°C lower temperature, and (ii) although the onset temperature of mullite formation is the same for both systems (1500°C/4 h), the volume fraction of mullite recorded is markedly higher in the fine-grain system. These observations lead to following conclusion: Since alumina dissolution is faster in the fine-grain system, owing to the much higher specific surface area, i.e. higher radius of curvature of the Al_2O_3 powder particles, the high Al-content in the siliceous phase initially retards nucleation and growth of cristobalite. Moreover, a fast Al-dissolution also strongly reduces the intrinsic glass viscosity, which in turn enhances cation diffusion through the siliceous phase. However, exceeding 1400°C, in both materials cristobalite formation was observed prior to the occurrence of mullite. Therefore, it is thought that cristobalite formation influences the mullitization reaction by indirectly affecting the Al-concentration of the siliceous phase. As soon as cristobalite nucleation in Si-rich regions and subsequent growth occurs, the Al-concentration of the residual glass markedly increases, which in turn favors mullite nucleation.

It should also be noted that in the coarse-grain system cristobalite is present up to a higher temperature (1600°C/0.5 h), which suggests that longer diffusion distances have to be overcome by Al_2O_3 and SiO_2 interdiffusion. This assumption is in principle in line

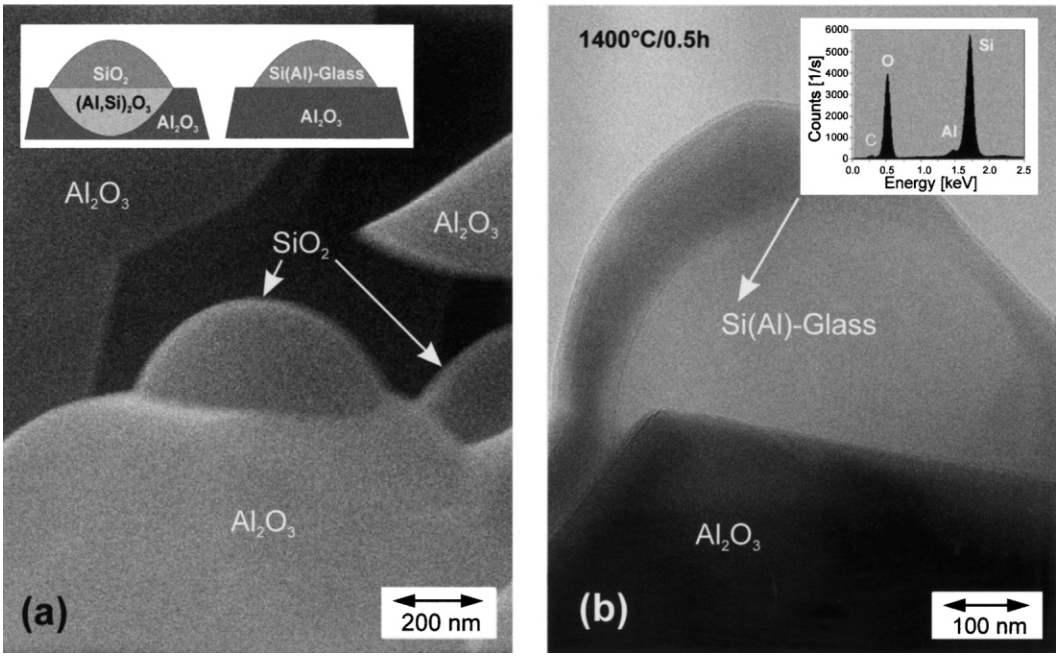

Fig. 8. (a) SEM image of a fracture surface of the coarse-grain system annealed at 1400°C, 0.5 h and (b) corresponding TEM image (1400°C, 0.5 h). Note that the initially isomorphic silica spheres became hemispheres. The SiO_2 glass contains some aluminum [see EDX inset in (b)], which is consistent with the dissolution of alumina in the siliceous phase [compare schematic shown in inset of (a)].

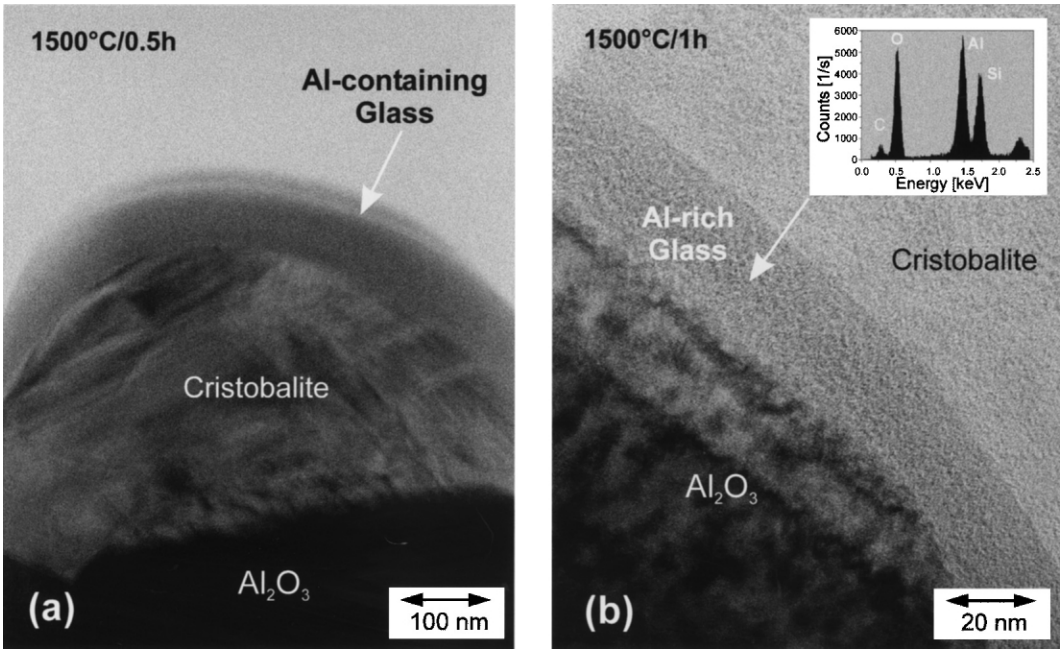

Fig. 9. TEM images of the coarse-grain system annealed at (a) 1500°C, 0.5 h and (b) 1500°C, 1 h. As shown in (a), the hemispheres (see also Fig. 8) are now composed of cristobalite and an Al-containing glass phase (on the outer surface). In (b) the formation of an additional Al-rich glass phase right at the Al_2O_3/cristobalite phase boundary is shown.

with results presented by Sacks et al.,[23] who reported that the 2nd stage of mullite formation was highly dependent on the initial composition. The reaction was completed at a much lower temperature in both Al_2O_3- and SiO_2-rich samples, as compared to a near stoichiometric composition, because shorter diffusion distances were effective in both non-stoichiometric materials. Although we do not compare different compositions here, the diffusion distances in the coarse-grain system are definitely longer, because the initial alumina particle size is about one order of magnitude larger. This also implies that the conversion rate of mullite formation is

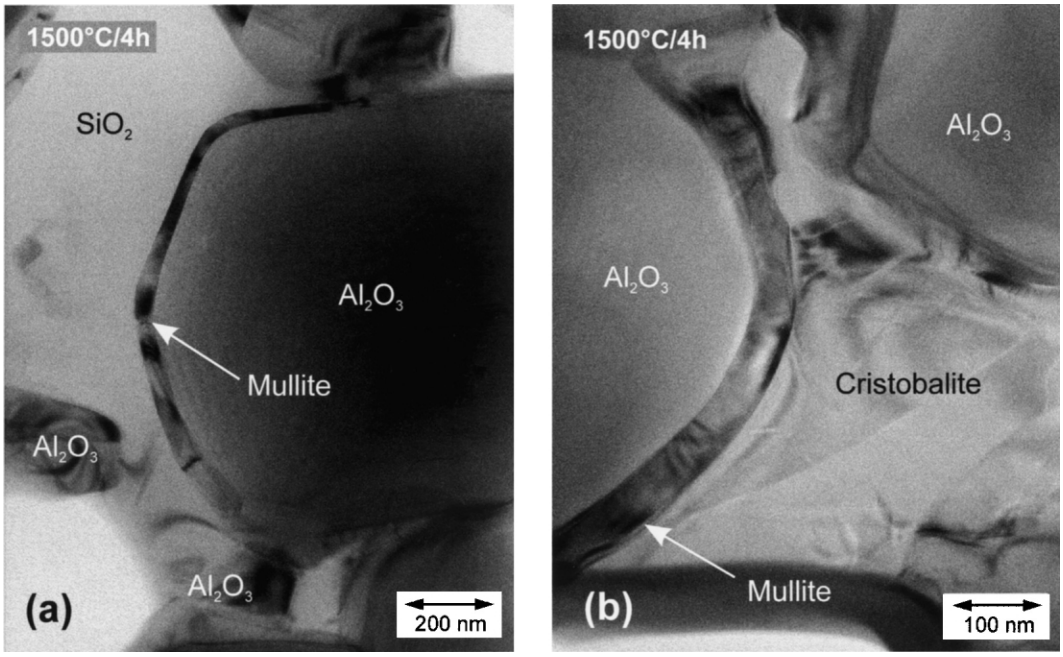

Fig. 10. TEM images (a) and (b) of the coarse-grain system annealed at 1500°C, 4 h. The Al-rich glass phase present at 1500°C, 1 h [shown in Fig. 9(b)] converted into a mullite coat surrounding the Al_2O_3 particles. Note that this coating resembles a mullite single crystal.

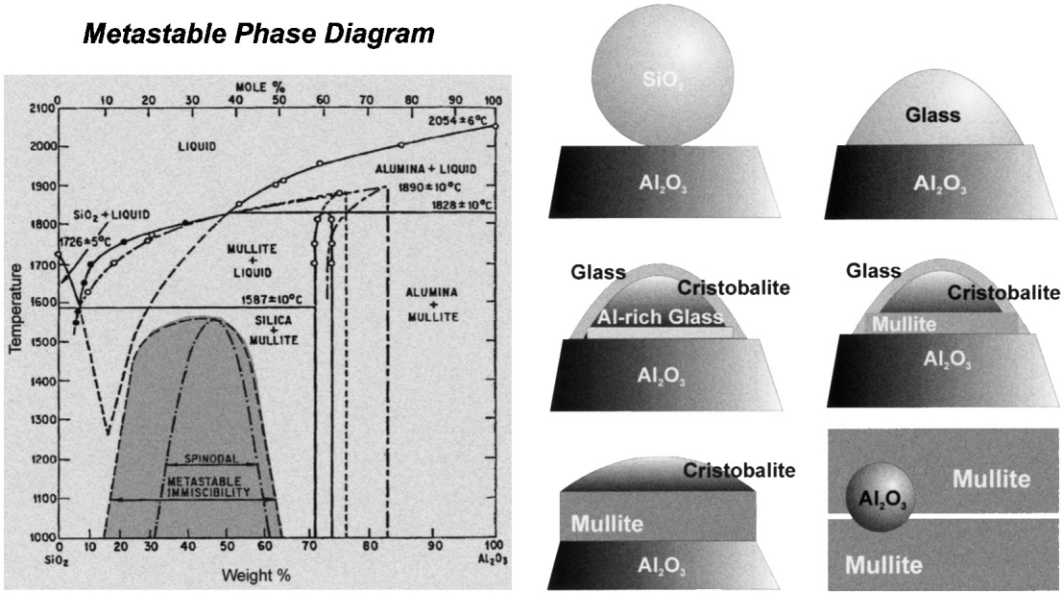

Fig. 11. Schematic illustrating the conversion mechanism of the coarse-grain system (heterogeneous nucleation), which follows the metastable phase diagram (after Aksay and Pask, 1975);[36] for further information it is referred to the text.

reduced, as determined by XRD analysis (compare Figs. 2 and 7).

These results emphasize the dependence of the transformation mechanism on the Al_2O_3 particle-diameter. Based on the Gibbs-Thompson effect,[35] the Al_2O_3 solubility within the siliceous glass phase is strongly affected by the intrinsic particle diameter:

$$C_r \approx C_\infty(1 + 2\gamma V_m/RTr) \quad (1)$$

where C_r is the solubility of the curved Al_2O_3 particle surface, C_∞ is the solubility of a planar alumina surface (with $r=\infty$) and γ is the solid–liquid interface energy. V_m stands for the molar volume, R and T are the gas constant and temperature, respectively, and r represents the Al_2O_3 particle radius. As can be seen from Eq. (1), a high radius of curvature, i.e. a small particle diameter, strongly enhances alumina dissolution and, hence, affects the respective conversion mechanism. Therefore,

the fine-grain system follows the stable phase diagram with homogenous nucleation and growth of mullite in the Al-containing glass. After a relatively short incubation time, a large amount of the material readily converted to mullite. However, one puzzling aspect of this study is that is was not possible to directly image the nucleation event of mullite even via HRTEM. Typically, the fine-grain material revealed either a phase assemblage of α-Al_2O_3/siliceous glass or the conversion reaction had already strongly progressed, so that mullite engulfing residual alumina particles in addition to some, however, isolated glass pockets were observed. Therefore, we repeated the experiment and prepared TEM-foils from the fine-grain system annealed at 1450°C/0.5 h and 1550°C/0.5 h, as shown in Fig. 12. These TEM micrographs clearly emphasize our earlier experimental finding that imaging the mullite nucleation event is rather difficult. As shown, extended glass pockets were found upon annealing at 1450°C/0.5 h [Fig. 12 (a)] which do not contain mullite nuclei. As shown in the inset, only a homogeneous glass phase was imaged by HRTEM, revealing a typical phase contrast of amorphous materials. Annealing at 1550°C for 0.5 h, only small isolated residual glass pockets were observed, which were completely surrounded by mullite matrix grains. This finding leads to the conclusion that, in the fine-grain system, mullite formation occurs rapidly and within a rather narrow temperature/time window. When reflecting the presented results, mullite formation could not be detected at 1400°C/0.5, 1500°C/0.5 and 1500°C/1 h, but mullitization had already strongly progressed during sintering at 1500°C/4 h or at 1550°C/0.5 h. Based on the 0.5 h holding time, rapid nucleation of mullite occurs between 1500 and 1550°C.

Although, for the reasons mentioned above, direct imaging of small mullite crystallites was not successful, we conclude that rapid, homogeneous nucleation within the alumino-silicate glass occurs. Moreover, due to both (i) small diffusion distances in conjunction with (ii) high diffusion rates (low glass viscosity owing to fast Al_2O_3 dissolution), growth of mullite crystallites in this 1st mullite formation stage is also very fast. This conclusion in consistent with experimental data obtained by Wei and Halloran[14,17] on their stoichiometric diphasic gels. They studied the phase transformation behavior and found that, after a temperature-dependent incubation time, a rapid nucleation event and subsequent fast mullite growth occurred. It is important to note that they also reported that mullite growth occurs from a constant nuclei density. This latter observation is in line with our experience: when reheating the TEM-foil of the 1500°C/4 h sample to 1550°C/0.5, only a slight increase in mullite grain size was monitored, in contrast to the expected formation of mullite nuclei within residual glass pockets.

Opposite to the fine-grain system, the coarse-grain system follows the metastable phase diagram.[27,36] At 1500°C, two different glass phases, one Al- and one Si-rich being present at (i) Al_2O_3/cristobalite phase boundary and (ii) SiO_2-hemisphere surface, respectively, were observed with cristobalite crystallizing in Si-rich regions (compare Fig. 9). A similar, metastable phase separation process was reported earlier in literature by Nurishi

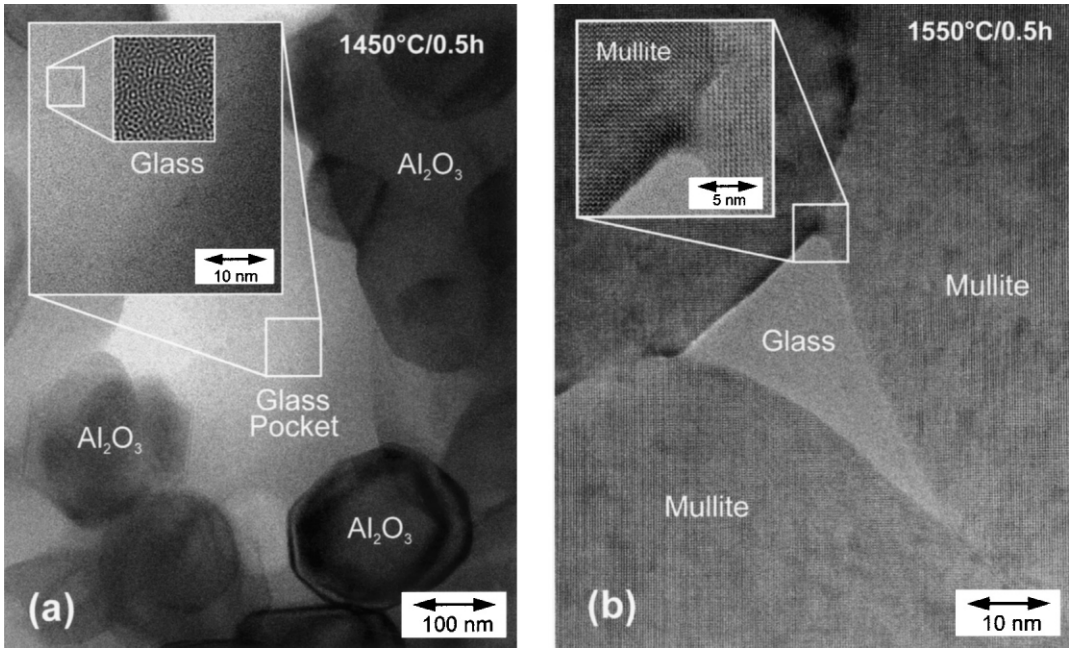

Fig. 12. TEM images of the fine-grain system annealed at (a) 1450°C, 0.5 h and (b) 1550°C, 0.5 h. In both cases, mullite nucleation within the siliceous phase could not be imaged by HRTEM. While in (a) extended glass phase pockets are still present that do not contain mullite nuclei (compare also insets), only small residual glass pockets are seen in (b), surrounded by relatively large mullite grains. It is concluded that rapid nucleation and growth of mullite occurs within the siliceous glass phase (narrow temperature/time window).

and Pask[25] and MacDowell and Beall.[37] Nurishi and Pask studied sintering of α-Al_2O_3/fused SiO_2 compacts and found that cristobalite, which crystallized from amorphous SiO_2, reacted with α-Al_2O_3 to form a metastable alumino-silicate liquid. Nucleation of cristobalite within this Al-containing glass phase was excluded since nucleation of mullite is instead favored. MacDowell and Beall observed a glass-in-glass separation by TEM (replica technique) on rapid quenching of Al_2O_3–SiO_2 melts.[37] They concluded that nucleation and subsequent growth of mullite occurs in the high-alumina-dispersed glass phase and that a metastable liquid immiscibility exists in the Al_2O_3–SiO_2 system. Moreover, Nurishi and Pask[25] reported on a second glass phase along the Al_2O_3/cristobalite phase boundary, however, they did not monitor mullite formation after heat treatment at 1500°C for 2 h. In our case, sintering at 1500°C for 2 h yielded consistent results, while 4 h annealing led to the transformation of the transient metastable glass film along the Al_2O_3/cristobalite phase boundary into mullite. Taking these literature data and our present results into account, the temperature/time window for mullitization can be narrowed down to 1500°C and $2 \leqslant t_{mul} \leqslant 4$ h.

It should be noted that in the Al-containing glass, existing on the surface of the former SiO_2 hemispheres [1500°C/0.5 h, Fig. 9(a)], no mullite formation was observed. It is assumed that this siliceous glass phase is stable up to high temperatures and will only be slowly consumed via interdiffusion. Therefore, in the coarse-grain model system, the Al_2O_3 particles are separated from the residual SiO_2-rich glass, and, consequently, only a thin reaction layer of mullite can be formed. The thickness of the mullite coat reflected the width of the metastable Al-rich glass film (≈30–50 nm). After mullite formation within the Al-rich glass, the Al_2O_3-particles and the residual siliceous glass are separated by mullite and subsequent grain growth is only possible by interdiffusion of Si^{4+} and Al^{3+} cations through the mullite coating.

The fine-grain system contained a higher amount of mullite, because nucleation proceeded in the Al-rich glass phase, while in the coarse-grain system only this thin layer of mullite is formed around the Al_2O_3 grains. HRTEM investigations of grain boundaries revealed no interfacial glass films in any of the systems. It is, therefore, concluded that mullite grain growth occurs by slow alumina/silica diffusion through bulk mullite grains, formed at the initial stage of transformation.

The diameter of the Al_2O_3 particles affects the conversion mechanisms in two ways. First, in the fine-grain material dissolution of Al_2O_3 is preferred, because of its higher specific surface area, i.e. the higher radius of curvature of the Al_2O_3 particles. Therefore, the fine-grain system follows the stable phase diagram as illustrated in Fig. 6. In contrast, the coarse-grain system follows the metastable phase diagram due to the formation of two metastable glass phases (SiO_2-hemisphere surface vs. Al_2O_3/cristobalite phase boundary) with different composition. Secondly, the diffusion distances during the final period of mullite formation are shorter in the fine-grain system, which favors both nucleation and growth of mullite.

It should be noted that when commercial powders are employed for processing of mullite components, a distinction between stable versus metastable conversion mechanism is no longer possible. Due to a commonly present wide Al_2O_3 grain-size distribution in commercially available powders, it is expected that both mechanisms occur simultaneously, as observed by Schmücker et al.,[30] who studied mullitization during reaction sintering of quartz and α-Al_2O_3 powders by transmission electron microscopy. They reported that nucleation of mullite mainly occurred at the α-Al_2O_3/silica melt contact (similar to the coarse-grain system studied here), however, to a minor amount within residual glass pockets (equivalent to our fine-grain system). In addition, since both microstructures obtained from the fine- and coarse-grain system were indistinguishable upon sintering at high temperature, a simultaneous occurrence of both conversion mechanisms can not easily be detected; an intrinsic advantage of such "model systems" employed here.

5. Conclusions

Two model systems were employed, both of which are composed of monosized powders, i.e. amorphous silica spheres (500 nm Ø) and crystalline α-Al_2O_3 particles with varying diameter (300 nm vs. 2 μm). The distinction between fine-grain and coarse-grain system is based on the difference in alumina particle diameter.

The fine-grain system is characterized by a fast dissolution of alumina in the viscous glass phase, promoted by the high curvature of the Al_2O_3 particles, followed by rapid nucleation and growth of mullite within the siliceous phase. When extended mullite regions are formed, further growth of mullite proceeds via interdiffusion of alumina and silica.

In contrast, the coarse-grain system revealed a different nucleation mechanism: here, two Al-containing glass phases with different composition were monitored. The Al-rich glass phase, which formed right at the Al_2O_3/cristobalite interface, developed into a single crystalline mullite coating that engulfed the alumina particles. Since dissolution of alumina is less favored in this system (larger particle size, reduced surface curvature), formation of cristobalite occurs at lower temperatures. This in turn favors the evolution of an Al-rich glass phase right at the Al_2O_3-particle surface, followed by heterogeneous nucleation of mullite at this phase boundary. It should be noted that prior to mullite formation, a separation of

the glass phase into a Si-rich and Al-rich glass was observed.

It is concluded that mullitization in these diphasic powder blends is dominated by different conversion mechanisms: while the fine-grain system follows the stable phase diagram with homogeneous nucleation within the siliceous glass phase, transformation in the coarse grain system occurs via the metastable phase diagram due to heterogeneous nucleation at phase boundaries. However, when commercial powder mixtures are employed, it is expected that both mechanisms occur simultaneously. This argument is supported by the observation that both microstructures, obtained from the fine- and coarse grain system, were indistinguishable upon annealing at temperatures exceeding 1600°C.

Here, for the first time, the validity of the proposed coexistence of the stable and metastable phase diagram, i.e. its applicability with reference to the $3Al_2O_3 + 2SiO_2 \Rightarrow$mullite conversion mechanism of powder mixtures, was verified by TEM imaging.

Acknowledgements

The authors would like to express their sincere thanks to Dr. W. Braue and Professor H. Schneider, DLR, Cologne, for numerous fruitful discussions. Sumitomo Chemical Co., Ltd., Tokyo, Japan is also greatly acknowledged for providing both monosized Al_2O_3 powders used here.

References

1. Bowen, N. L., Greig, J. W. and Zies, E. G., Mullite, a silicate of alumina. *J. Wash. Acad. Sci.,* 1924, **14**(9), 183–194.
2. Bowen, N. L. and Greig, S. W., The system Al_2O_3–SiO_2. *J. Am. Ceram. Soc.,* 1924, **7**, 238–241.
3. Ohira, H., Shiga, H., Ismail, M. G. M. U., Nakai, Z., Akiba, T. and Yasuda, E., Compressive creep of mullite ceramics. *J. Mater. Sci. Letters,* 1991, **10**, 847–849.
4. Hynes, A. P. and Doremus, R. H., High temperature compressive creep of polycristalline mullite. *J. Am. Ceram. Soc.,* 1991, **74**(10), 2469–2475.
5. Tummala, R. R., Ceramic and glass-ceramic packaging in the 1990s. *J. Am. Ceram. Soc.,* 1991, **74**(5), 895–908.
6. Rhanim, H., Olagnon, C., Fantozzi, G. and Torrecillas, R., Experimental characterization of high temperature creep resistance of mullite. *Ceram. Int.,* 1997, **23**, 497–507.
7. Schneider, H., Rodewald, K. and Eberhard, E., Thermal expansion discontinuities of mullite. *J. Am. Ceram. Soc.,* 1993, **76**(11), 2896–2898.
8. Osendi, M. I. and Baudin, C., Mechanical properties of mullite materials. *J. Eur. Ceram. Soc.,* 1996, **16**, 217–224.
9. Mah, T.-L. and Mazdiyasni, K. S., Mechanical properties of mullite. *J. Am. Ceram. Soc.,* 1983, **66**(10), 699–703.
10. Dokko, P. C., Pask, J. A. and Mazdiyasni, K. S., High temperature mechanical properties of mullite under compression. *J. Am. Ceram. Soc.,* 1983, **66**(10), 699–703.
11. Ohnishi, H., Kawanami, T., Nakahira, N. and Niihara, K., Microstructure and mechanical properties of mullite. *Yogyo Kyokaishi,* 1990, **98**(6), 541–547.
12. Schneider, H., Okada, K. and Pask, J. A., *Mullite and Mullite Ceramics.* Wiley, Chichester, UK, 1994.
13. Li, D. X. and Thomson, W. J., Mullite formation kinetics of a single-phase gel. *J. Am. Ceram. Soc.,* 1990, **73**(4), 964–969.
14. Wei, W.-C. and Halloran, W. J., Phase transformation of diphasic alumosilicate gels. *J. Am. Ceram. Soc.,* 1988, **71**(3), 166–172.
15. Huling, J. C. and Messing, G. L., Epitactic nucleation of spinel in aluminum silicate gels and effect on mullite crystallization. *J. Am. Ceram. Soc.,* 1991, **74**(10), 2374–2381.
16. Sacks, M. D., Wang, K., Scheiffele, G. W. and Bozkurt, N., Mullitization behavior of alpha alumina/silica microcomposite powders. In *Ceramic Microstructures '96*, ed. A. P. Tomsia and A. M. Glaeser. Plenum Press, 1998, pp. 285–301.
17. Wei, W.-C. and Halloran, W. J., Transformation kinetics of diphasic aluminum silicate gels. *J. Am. Ceram. Soc.,* 1988, **71**(7), 581–587.
18. Kara, F., Turan, S., Little, J. A. and Knowles, K. M., Microstructural characterization of reactively sintered mullites. *J. Am. Ceram. Soc.,* 2000, **83**(2), 369–376.
19. Li, D. X. and Thomson, W. J., Kinetic mechanisms for the mullite formation from sol-gel precursors. *J. Mater. Res.,* 1990, **5**(9), 1963–1969.
20. Sundaresan, S. and Aksay, I. A., Mullitization of diphasic aluminosilicate gels. *J. Am. Ceram. Soc.,* 1991, **74**(10), 2388–2392.
21. Sacks, M. D., Bozkurt, N. and Scheiffele, G. W., Fabrication of mullite and mullite-matrix composites by transient viscous sintering of composite powders. *J. Am. Ceram. Soc.,* 1991, **74**(10), 2428–2437.
22. Sacks, M. D., Wang, K., Scheiffele, G. W. and Bozkurt, N., Activation energy for mullitization of alpha aluminas/silica microcomposite particles. *J. Am. Ceram. Soc.,* 1996, **79**(2), 571–573.
23. Sacks, M. D., Wang, K., Scheiffele, G. and Bozkurt, N., Effect of composition on mullitization behavior of α-alumina/silica microcomposite powders. *J. Am. Ceram. Soc.,* 1997, **80**(3), 663–672.
24. Wahl, F. M., Grim, R. E. and Graf, R. B., Phase transformations in silica-alumina mixtures as examined by continuous X-ray diffraction. *The American Mineralogist,* 1961, **46**(9-10), 1064–1076.
25. Nurishi, Y. and Pask, J. A., Sintering of α-Al_2O_3-amorphous silica compacts. *Ceram. Int.,* 1982, **8**(2), 57–59.
26. Rana, A., Aiko, O. and Pask, J. A., Sintering of α-Al_2O_3-/quartz and Al_2O_3/cristobalite related to the mullite formation. *Ceram. Int.,* 1982, **8**(2), 151–156.
27. Risbud, S. H. and Pask, J. A., SiO_2–Al_2O_3 metastable phase equilibrium diagram without mullite. *J. Mater. Sci.,* 1978, **13**(11), 1449–1454.
28. Sosman, R. B., *The Phases of Silica.* Rutgers Univ. Press, New Brunswick, NJ, 1965.
29. Johnson, S. M. and Pask, J. A., Role of impurities on formation of mullite from kaolinite and Al_2O_3–SiO_2 mixtures. *Ceram. Bull.,* 1982, **61**, 838–843.
30. Schmücker, M., Albers, W. and Schneider, H., Mullite formation by reaction sintering of quartz and α-Al_2O_3 — a TEM study. *J. Eur. Ceram. Soc.,* 1994, **14**, 511–515.
31. Takamori, T. and Roy, R., Rapid crystallization of SiO_2–Al_2O_3 glasses. *J. Am. Ceram. Soc.,* 1973, **56**(12), 639–644.
32. Giesche, H., Synthesis of monodispersed silica powders; I. Particle properties and reaction kinetics. *J. Eur. Ceram. Soc.,* 1994, **14**, 189–204.
33. Giesche, H., Synthesis of monodispersed silica powders; ii. Controlled grain growth reaction and continuous production process. *J. Eur. Ceram. Soc.,* 1994, **14**, 205–214.

34. Kleebe, H.-J., Hilz, G. and Ziegler, G., TEM and EELS characterization of the glass phase in sol-gel derived mullite. *J. Am. Ceram. Soc.,* 1996, **79**(10), 2592–2600.
35. Porter, D. A. and Easterling, K. E., Phase transformations in metals and alloys. 2nd edn. Chapman and Hall, New York, 1992, pp. 1–59.
36. Aksay, I. A. and Pask, J. A., Stable and metastable phase equilibria in the system Al_2O_3/SiO_2. *J. Am. Ceram. Soc.,* 1975, **58**(11–12), 507–512.
37. MacDowell, J. F. and Beall, G. H., Immiscibility and crystallization in Al_2O_3–SiO_2 glasses. *J. Am. Ceram. Soc.,* 1969, **52**(1), 17–25.